arXiv:1301.3368v1 [nucl-ex] 15 Jan 2013

Investigation of activation cross-sections of proton induced nuclear reactions on ^{nat}Tl up to 42 MeV: review, new data and evaluation

F. Tárkányi[a], F. Ditrói[a,*], A. Hermanne[b], S. Takács[a], R. Adam-Rebeles[b], N. Walravens[b], O. Cichelli[b], A.V. Ignatyuk[c]

[a] *Institute of Nuclear Research of the Hungarian Academy of Sciences (ATOMKI), Debrecen, Hungary*
[b] *Cyclotron Laboratory, Vrije Universiteit Brussel (VUB), Brussels, Belgium*
[c] *Institute of Physics and Power Engineering (IPPE), Obninsk, Russia*

Abstract

Cross-sections of proton induced nuclear reactions on natural thallium have been studied for investigation of the production of the medical important ^{201}Tl diagnostic radioisotope. The excitation functions of ^{204m}Pb, ^{203}Pb, ^{202m}Pb, ^{201}Pb, ^{200}Pb, ^{199}Pb, ^{202}Tl (direct, cumulative), ^{201}Tl (direct, cumulative), ^{200}Tl(direct), and ^{203}Hg were measured up to 42 MeV proton energy by stacked foil technique and activation method. The experimental data were compared with the critically analyzed experimental data in the literature, with the IAEA recommended data and with the results of model calculations by using the ALICE-IPPE, EMPIRE-II and TALYS codes.

Keywords: Tl targets, proton induced reactions, experimental cross-sections, model calculations, Pb, Tl and Hg radioisotopes, medical radionuclides

1. Introduction

The radionuclide ^{201}Tl ($T_{1/2} = 73h$) as a good potassium analog has been used widely in diagnostic nuclear medicine for forty years (Qaim, 2001). ^{201}Tl decays by EC (100%) and emits a 167 keV γ-ray used for SPECT imaging. The ^{201}Tl can be produced at charged particle accelerators. The investigated nuclear reactions are collected in Table. 1 (Adam-Rebeles et al., 2012; Al-Saleh et al., 2007; Bell and Skarsgard, 1956; Birattari et al., 1982; Blue et al., 1978; Comar and Crouzel, 1975; Dmitriev et al., 1976; Fernandes and da Silva, 1992; Gloris et al., 2001; Hermanne et al., 1992; Kuhnhenn et al., 2001; Lagunas-Solar et al., 1980, 1981, 1978; Lebowitz et al., 1975; Nayak et al., 2002; Qaim et al., 1979; Sakai et al., 1965; Zaitseva et al., 1987). The theoretical excitation functions for the most important routes are shown in Fig. 1.

The final result of these studies and of the everyday practice is that the $^{203}Tl(p,3n)^{201}Pb \longrightarrow^{201} Tl$ production route appears to be the most practical one taking into account the targetry, the production yields, the available accelerators, the radionuclide purity, etc. Presently the $^{203}Tl(p,3n)$ reaction is used exclusively for production of ^{201}Tl. In the next chapters we are discussing only this production route together with side reactions during bombardment of thallium target with protons. In Table 2 we have collected the most important physical parameters of the experiments related to the measurement of activation cross-section and yield of proton induced nuclear reactions on thallium (Al-Saleh et al., 2007; Blue et al., 1978; Bonardi, 1987; Dmitriev

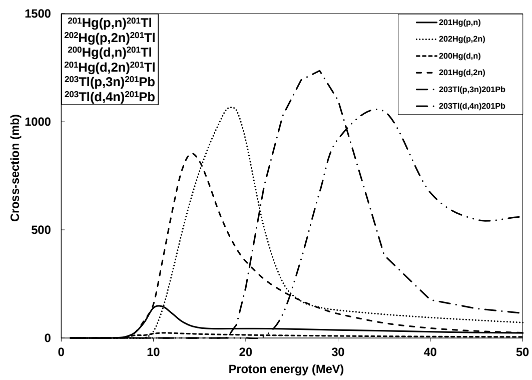

Figure 1: Excitation functions (TENDL 2011) of the most important nuclear reactions for production of ^{201}Tl

*Corresponding author: ditroi@atomki.hu

Table 1: Investigated nuclear reactions for production of ^{201}Tl

Reaction	References	Comment
^{203}Tl(p,3n)^{201}Pb$\longrightarrow$ ^{201}Tl	Sakai (Sakai et al., 1965) Lebowitz (Lebowitz et al., 1975) Blue (Blue et al., 1978) Lagunas-Solar (Lagunas-Solar et al., 1978) Qaim (Qaim et al., 1979) Bonardi (Birattari et al., 1982) Hermanne (Hermanne et al., 1992) Al-Saleh (Al-Saleh et al., 2007)	Only presently used in practice
^{205}Tl(p,xn)^{201}Pb$\longrightarrow$^{201}Tl	Lagunas-Solar (Lagunas-Solar et al., 1980)	Requires high energy beam
^{203}Tl(d,4n)^{201}Pb$\longrightarrow$^{201}Tl	Adam Rebles (Adam-Rebeles et al., 2012) Blue (Blue et al., 1978)	Requires high energy beam
^{201}Hg(p,n)^{201}Tl	Fernandes (Fernandes and da Silva, 1992) Comar (Comar and Crouzel, 1975)	Low cross-section
^{202}Hg(p,2n)^{201}Tl	Birattari (Birattari et al., 1982)	^{202}Tl impurity level
^{200}Hg(d,n)^{201}Tl ^{201}Hg(d,2n)^{201}Tl	Dmitriev (Dmitriev et al., 1976) Comar (Comar and Crouzel, 1975)	Low cross-section ^{202}Tl impurity level
^{nat}Pb(p,x)^{201}Tl	Zaitseva (Zaitseva et al., 1987) Lagunas-Solar (Lagunas-Solar et al., 1981) Gloris (Gloris et al., 2001; Kuhnhenn et al., 2001) Bell (Bell and Skarsgard, 1956)	Requires high energy beam
^{197}Au(^{7}Li,p2n)^{201}Tl	Nayak (Nayak et al., 2002)	Easy targetry Poor availability of ^{7}Li beam
^{197}Au(^{6}Li,pn)^{201}Tl		Easy targetry Poor availability of ^{6}Li beam

et al., 1976; Hanna et al., 1977; Hermanne et al., 1992; Kernert et al., 1983; Lagunas-Solar et al., 1978; Lebowitz et al., 1975; Malinin et al., 1984; Milazzo-Colli et al., 1975; Qaim et al., 1979; Sakai et al., 1965; Sattari et al., 2003). According to Table 2, a large number of papers was published on $Tl(p,x)^{201}Pb \longrightarrow^{201} Tl$ production and chemistry, on compilation of the earlier experimental data and on the calculation of cross-section by using different theoretical model codes. In Table 3 we have summarized the most important compilations and theoretical calculations (Canderias-Cruz and Okamoto, 1987; Dmitriev and Zaitseva, 1996; Groppi et al., 2001; Haji-Saeid et al., 2009; Hermanne et al., 2001; Iljinov et al., 1993; Kaplan et al., 2009; Koning and Rochman, 2011; Kurenkov et al., 1995; Lagunas-Solar et al., 1978; Mihailescu et al., 2007; Nowotny, 1981; Rurarz, 1994; Sheu et al., 2003; Shubin, 2001; Shubin et al., 1998; Szelecsényi et al., 1995; Takács et al., 2005; Tel et al., 2011). In spite of numerous earlier works we decided to make new measurements and new evaluations on the activation cross-sections of proton induced reactions on thallium. The aim of the present study and the report was manifold:

1. Some part of the recently reported experimental data were measured long time ago (Hermanne et al., 1992). Only preliminary results were reported in equidistant energy scale obtained by fitting the experimental data, without any details on experiments and on the nuclear data used for the data evaluation. This fitted preliminary data were used for preparation of recommended data file of IAEA (Hermanne et al., 2001) for production of ^{201}Tl and used in the upgraded data library (Takács et al., 2005) without correction of the decay data. In this work we decided to publish the original experimental data corrected with upgraded decay data for further use to prepare recommended data (see this work - ser. 1).
2. During the last decade new experiments were performed, which could be included into the new evaluation. It is necessary to check the earlier works in respect of new monitor and decay data.
3. The theoretical model codes were significantly improved in the last decade and new input parameter library was developed. It was a challenge to see the predictivity of these codes in comparison with the experimental data and with the earlier model results.
4. We have performed experiments on deuteron induced reactions on ^{nat}Tl up to 50 MeV (Adam-Rebeles et al., 2011). We thought it is worthwhile to repeat the experiments with proton beam using the same experimental technology (target preparation, spectra measurements, etc.).
5. Last but not least in connection with investigation of production possibility of ^{201}Tl in Hungary, the ATOMKI group had direct practical interest in the targetry and the production yields (similar to the case of other routinely produced isotopes (^{11}C, ^{18}F, ^{67}Ga, ^{111}In, ^{123}I). In such a way, to complete our systematical study of excitation functions for production of medical radioisotopes and to make new evaluation we decided to make new measurement relative to the well-established monitor reactions by using more modern experimental and eval-

uation techniques (see this work ser. 2).

2. Experimental

We have performed two series of experiments. The first series was measured 20 years ago and the second was done in the last year.

2.1. Experimental and data evaluation details of the first series of measurements:

Samples of natural Tl (50 μm) were prepared by electroplating on brass-foils (50 μm). No additional monitoring foils were inserted into the stacks. The irradiation was done at the VUB CGE 560 cyclotron at beam current of 3-6 μA, for 3-6 minutes. 13 stacks of 7-12 foils were irradiated at incident energies of 43-22 MeV. The number of incident particles was determined from the integrated charge measured in Faraday cup. Tl produced in irradiated samples was quantitatively dissolved after irradiation and aliquots of 1 ml sample were measured using a Ge(Li) detector calibrated with reference sources of ^{22}Na, ^{152}Eu, ^{60}Co (2% error on standards). The proton energy degradation along the stack was computed using the stopping formulae coefficients of Andersen and Ziegler for Tl (Andersen and Ziegler, 1977) and the tabulated stopping powers of (Janni, 1966) for the brass backings. The production cross-section was calculated from activity. Quadratic summation of the uncertainties of the contributing parameters results an absolute error of 8.5% (target thickness (2%), detector efficiency (5%), physical decay data (5%), integrated beam current (2%), counting statistics (2%)). Nuclear decay data originally were taken from Erdtmann and Soyka (Erdtmann and Soyka, 1979). For preparation of the IAEA recommended data base (Takács et al., 2005) and for compilation into the EXFOR format the decay data were corrected according to the newest parameters (Browne and Firestone, 1986). In the recent work the cross-section data were corrected according to the new decay data, and the uncertainty of the number of incident particle on the basis of comparisons of the monitor reactions and the Faraday cup data was enlarged from 2 % to 7 %, resulting in 11 % total uncertainty. The results of the earlier data evaluation were corrected for the recent recommended data of the γ-ray intensities. No corrections were done for the half-lives (nonlinearly contributing factor), but there are only small changes in half-lives. In a few cases there are significant changes in γ-ray intensities (see Table 4). There are significant changes in decay data for ^{201}Pb, ^{200}Pb used by Lagunas Solar et al., for 401 keV γ-line of ^{203}Pb used by Al Saleh et al. (Al-Saleh et al., 2007). In the case of the ^{199}Pb the recent decay data also differ significantly from data used by Hermanne et al. (Hermanne et al., 1992) and by Qaim et al. (Qaim et al., 1979). The correction for the decay data is complicated when the authors used many γ-lines, for which different corrections are required according to the recent data. In this case the correction was done for the strongest γ-line. It should be mentioned that the automatic corrections of the of the cross-section and yield data for the new decay data is not a simple question in the case of many used γ-lines, taking into account the lack of the information in the original publications on the averaging of cross-section data obtained from different γ-lines, measured at different time, sometimes at different sample - detector distances.

2.2. Experimental and data evaluation details of the second series of measurement:

Samples of natural Tl were prepared also by electroplating. Simultaneous plating of four 15 μm thallium target layers (surface area 11.69 cm^2) on 12.5 μm Cu foil were used. The plating method is described in detail in (Afarideh et al., 2004). The electroplated foils for preparation of target stack were cut for 10x10 mm pieces. No additional monitoring foils were inserted into the stacks, the nuclear reactions induced on the backing Cu foils were used as beam monitors. The irradiation was done at VUB CGE 560 cyclotron in a short Faraday cup at beam current 90 nA, for 75 minutes irradiation for time, at 37 MeV incident energy. The radioactivity of the irradiated sample and monitor foils was measured nondestructively using HPGe γ-spectrometry. Counting was started about 3-4 hours after the end of the bombardment (EOB). The proton energy degradation along the stack was computed using the stopping formulae coefficients of Andersen and Ziegler for Tl (Andersen and Ziegler, 1977), and corrected on the basis of a simultaneously measured $^{nat}Cu(p,x)^{62}Zn,^{65}Zn$ monitor reactions (Tárkányi et al., 2001).The uncertainties in the energy scale were estimated taking into account the uncertainty of the energy of the primary beam, the calculated beam straggling and the measures necessary for the energy corrections on the basis of simultaneously measured excitation functions of monitor reactions.

The intensity of the incident beam was obtained from the charge collected in a Faraday cup and corrected using the monitor reactions. The best agreement was found after small corrections on the beam intensity (7% with respect to the Faraday cup results) and on the primary beam energy (0.5 MeV). According to the Fig.

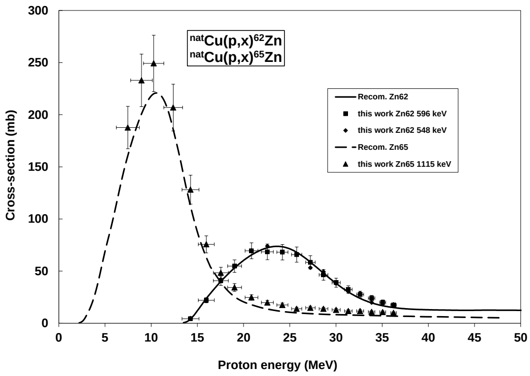

Figure 2: Application of monitor reactions for determination of proton beam energy and intensity

2 the agreement is good in the whole energy range. The production cross-section was calculated from activity. So called "elemental" cross-sections were determined, considering that the Tl targets are monoisotopic. The decay data were taken from NuDat database (NuDat, 2011) the reaction Q-values from (Pritychenko and Sonzogni, 2003) . The used decay data are summarized in Table 5. The uncertainties were estimated in the standard way (of-Weights-and Measures, 1993) by combining the individual errors in quadrature. The main sources of error were: beam current (8%), counting statistics and peak area determination (1-7%), detector efficiency (5%), decay data (3%) and effective target thickness (5%)). A total uncertainty of 12-20% is obtained.

3. Theoretical calculations

The measured cross-sections were compared to theoretical effective cross-sections calculated by using the ALICE-IPPE (Dityuk et al., 1998) and EMPIRE-II (Herman et al., 2007)(codes as well as with the data based on the latest version of the TALYS code (Koning et al., 2007), retrieved from the online TENDL 2011 file (Koning and Rochman, 2011). An a priori calculation was done without any knowledge of the experimental results and thus without any parameter adjustment. For each activation product the reaction cross-section on the individual target isotopes was calculated and a weighted summation (according to the abundance of natural occurrence) was made to obtain the total production cross-section.

4. Results

4.1. Excitation functions

The cross-sections for all the reactions studied are shown in Figures 3 - 13 and the numerical values are collected in Tables 6 - 8. The results of the two series of measurements are shown separately. Our results of the two series of measurements are in acceptable good agreement. In most cases the radioisotopes are formed via nuclear processes occurring on ^{203}Tl and ^{205}Tl. The cross-sections presented here refer to so called effective "elemental" cross-sections, calculated on hypothetic monoisotopic thallium target having number of target nuclei equal to the number of the sum of the numbers of ^{205}Tl and ^{207}Tl isotopes. We discuss the different reaction products individually.

4.1.1. Activation cross-sections of lead radioisotopes

The radioisotopes of lead are produced via (p,xn) reactions on ^{203}Tl and ^{205}Tl. The earlier experimental activation data on Tl are related mainly to the production of radioisotopes of lead, and was measured mostly up to 40 MeV.

$^{nat}Tl(p,xn)^{204m}Pb$ **reaction**

This radioisotope has two states: a shorter-lived ($T_{1/2}$ = 66.93 m, $I^{\pi} = 9^{-}$) decaying by IT to the ground state. The only reaction leading to the formation of ^{204m}Pb from natural thallium is the $^{205}Tl(p,2n)$ reaction (if we neglect the small contribution from $^{203}Tl(p,\gamma)$). The calculations with various codes are compared with the present- and the literature experimental data are shown in Fig. 3. The experimental data show acceptable good agreement with the theory (except Lagunas Solar (Lagunas-Solar et al., 1978) data). Systematic energy shift to the higher energies can be observed for experimental data of Al-Saleh (Al-Saleh et al., 2007). No TENDL calculated data are presented for production of ^{204m}Tl, only for total production cross-section of ^{204}Tl.

$^{nat}Tl(p,xn)^{203}Pb$ **reaction**

The ^{203}Pb radioisotope is formed by $^{203}Tl(p,n)^{203}Pb$ and $^{205}Tl(p,3n)^{203}Pb$ reactions. The contributions of the reactions are well separated in Fig. 4. The available experimental data are in good agreement, except the data of Lagunas-Solar (Lagunas-Solar et al., 1978) and Sakai (Sakai et al., 1965) (see Fig. 4). The theoretical data in TENDL 2011 describe well the experimental results.

$^{nat}Tl(p,xn)^{202m}Pb$ **reaction**

The experimental and theoretical data for production of ^{202m}Pb are shown in Fig. 5. We were able to measure the production cross-section only of the shorter-lived metastable state (3.5 h), which decays mostly

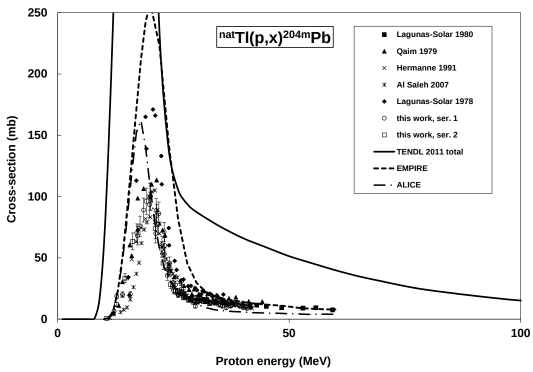

Figure 3: Excitation function of $^{nat}Tl(p,x)^{204m}Pb$ reaction

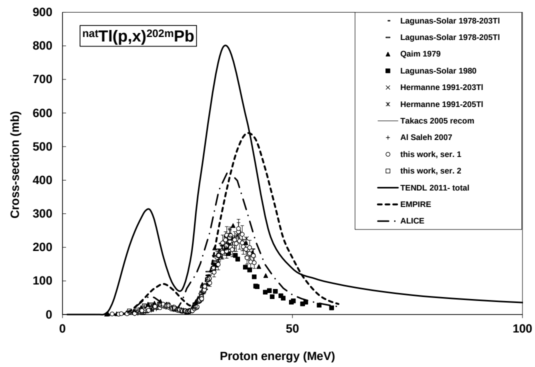

Figure 5: Excitation function of $^{nat}Tl(p,x)^{202m}Pb$ reaction

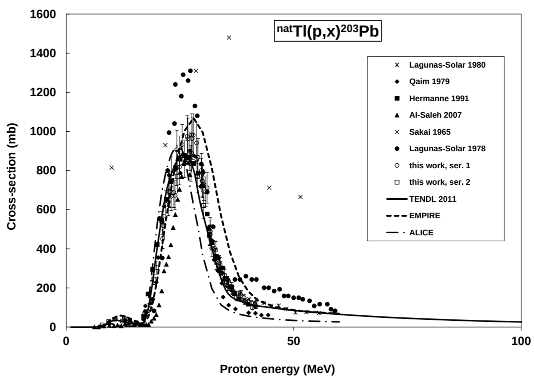

Figure 4: Excitation function of $^{nat}Tl(p,x)^{203}Pb$ reaction

(90.5%) by internal transition to the longer-lived (5250 a) ground state. In the investigated energy range both the $^{203}Tl(p,2n)$ and the $^{205}Tl(p,4n)$ contribute to the formation of ^{202m}Pb isomeric state. The comparison of the experimental data shows generally good agreement. At low energies the experimental data of Lagunas Solar (Lagunas-Solar et al., 1978) and (Al-Saleh et al., 2007) shows energy shift towards high energies. There are no theoretical data in the TENDL 2011 for isomeric states, only for the total production of ^{202}Pb.

$^{nat}Tl(p,xn)^{201}Pb$ **reaction**

The obtained new data are shown in Fig. 6 in comparison with the literature experimental data and with the theory. The structure of the excitation function (similar to previous processes) shows two maxima in the investigated energy range. The origin of the first peak is the $^{203}Tl(p,3n)^{201}Pb$ process. The second peak is due to the (p,5n) process on ^{205}Tl. Our data in maximum is in good agreement with the results of Lagunas Solar (Lagunas-Solar et al., 1978) , data of Bonardi measured on enriched target (Bonardi et al., 1982), of Al-Saleh (Al-Saleh et al., 2007) and Qaim (Qaim et al., 1979). It should be mentioned that the data of Qaim (Qaim et al., 1979) are very scattered with approximately 30% difference at the same energies (having 10-15% uncertainties). Our data support the results of higher values (the low and high energy data came probably from beam current measurement of irradiations of different stacks). As it was mentioned at the previous reactions, the Al-Saleh data (Al-Saleh et al., 2007) are shifted in energy near the threshold. The calculated cross-section curve follows the general trend of the experimental data.

$^{nat}Tl(p,xn)^{200}Pb$ **reaction**

Irradiating thallium targets having natural isotopic composition the $^{203}Tl(p,4n)$ (Q = -24514.2 keV) and the $^{205}Tl(p,6n)$ (Q = -38716.2 keV) reaction contribute to the production of ^{200}Pb. According to Fig. 7 the agreement of experimental data is acceptable good, except the scattered data of Sakai et al (Sakai et al., 1965), and the contradicting data of Lagunas-Solar at high energies reported in (Lagunas-Solar et al., 1978) and his derived data (Lagunas-Solar et al., 1981). The theoretical data in TENDL 2011 describe well the low energy part where reliable experimental data exist.

$^{nat}Tl(p,xn)^{199}Pb$ **reaction**

In the investigated energy range only the $^{203}Tl(p,5n)$ process contributes to the production of ^{199}Pb. Only one earlier data set was found in the literature, reported

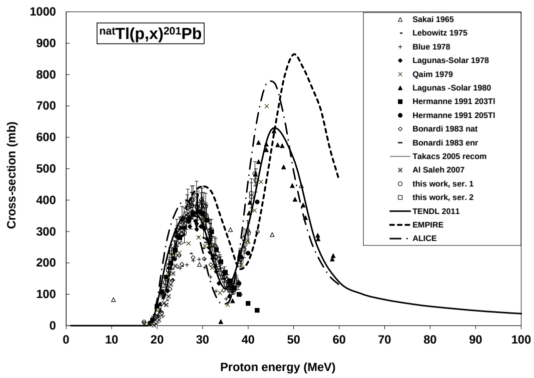

Figure 6: Excitation function of $^{nat}Tl(p,x)^{201}Pb$ reaction

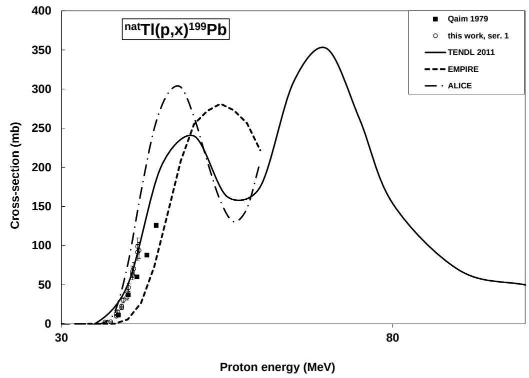

Figure 8: Excitation function of $^{nat}Tl(p,x)^{199}Pb$ reaction

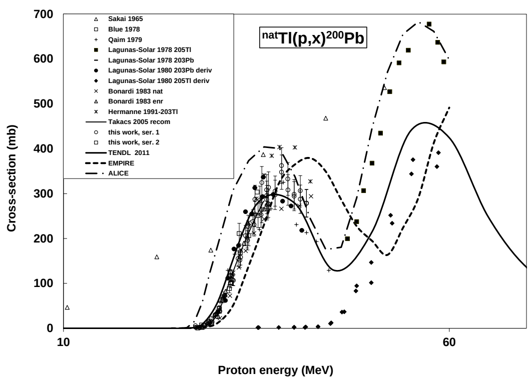

Figure 7: Excitation function of $^{nat}Tl(p,x)^{200}Pb$ reaction

by Qaim et al (Qaim et al., 1979). Our new data show acceptable agreement with these experimental data and with the prediction of TALYS calculation in TENDL 2011 (see Fig. 8).

4.1.2. Activation cross sections of thallium radioisotopes

The radioisotopes of thallium are formed directly via (p,pxn) reaction and through the decay of parent lead radioisotopes.

$^{nat}Tl(p,xn)^{202}Tl$ **reaction**

Parallel with the direct production the radioisotope is produced indirectly via the decay of the ^{202m}Pb ($T_{1/2}$ = 3.54 h, EC(9.5%)) and of the decay of the long-lived ^{202g}Pb ($T_{1/2}$ = 52.5E+3 a, EC(100%)). The cross-sections were calculated from spectra measured few days after EOB i.e. after complete decay of ^{202m}Pb, but insignificant decay of ^{202g}Pb. In such a way our cumulative cross-sections contain contributions from the direct decay of ^{202m}Pb. In Fig. 9 we show our cumulative data and corrected data for direct production of ^{202}Tl (when the contribution from the ^{202m}Pb were subtracted). For comparison we also present the experimental data of Qaim (Qaim et al., 1979) corrected for the contribution of ^{202m}Pb decay (direct cross-sections), and the theoretical data for the direct production. The comparison shows good agreement with the earlier data and with theory.

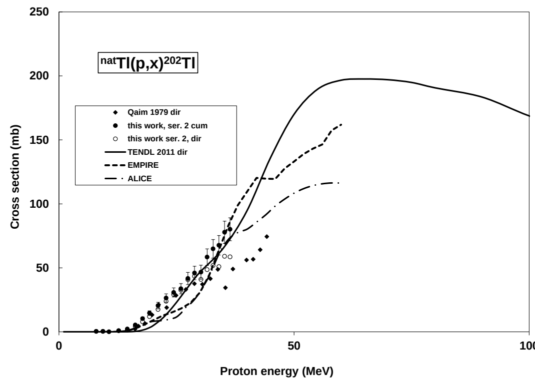

Figure 9: Excitation function of $^{nat}Tl(p,x)^{202}Tl$ reaction

$^{nat}Tl(p,xn)^{201}Tl$ **reaction**

The ^{201}Tl ($T_{1/2}$ = 3.0421 d) radioisotope is formed directly through the $^{203}Tl(p, p2n)$, and $^{205}Tl(p, p4n)$ reactions and indirectly from the decay of $^{201}Pb(T_{1/2}$ = 9.33 h). In Fig. 10 we present cumulative cross-section of ^{201}Tl after complete decay of ^{201}Pb, and cross-section for direct production when the contribution from the decay of parent was subtracted. Our direct production cross-section data are systematically higher compared to the results of Qaim (Qaim et al., 1979). The uncertainty of direct production is large, taking into account the large contribution of the parent.

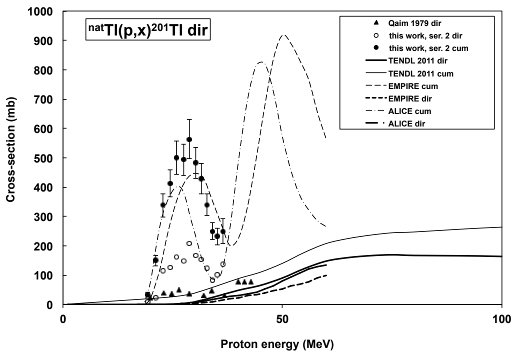

Figure 10: Excitation function of $^{nat}Tl(p, x)^{201}Tl$ reaction

$^{nat}Tl(p, xn)^{200}Tl$ reaction

In Fig. 11 we present direct production cross-section for production of ^{200}Tl ($T_{1/2}$ = 26.1 h) after subtraction the contribution of the indirect production through the decay of ^{200}Pb ($T_{1/2}$ = 21.5 h). We have only a few points near the threshold and the uncertainties are high due to the high contribution of the parent.

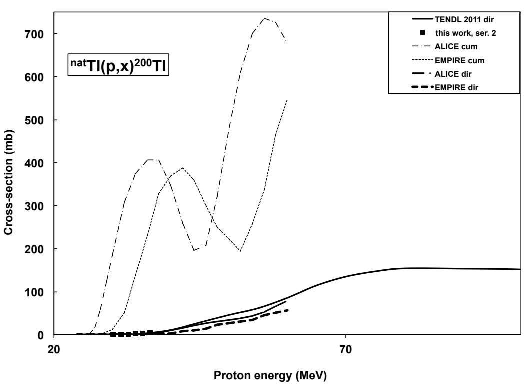

Figure 11: Excitation function of $^{nat}Tl(p, x)^{201}Tl$ reaction

4.1.3. Activation cross-sections of mercury radioisotopes

The radioisotopes of mercury are formed directly via (p,2pxn) reaction and through the decay of parent lead radioisotopes. We could measure activation cross-section only for production of ^{203}Pb. In principle the thresholds for production of ^{199m}Hg (42.67 min, IT: 100%), ^{197m}Hg (23.8 h, IT: 91.4%) and ^{197g}Hg (64.14 h , EC 100%) are lower than our maximum energy, but due to the low cross-sections (theoretical estimation in Fig. 12), to the weak γ-lines and to the short half-life no reliable data were found.

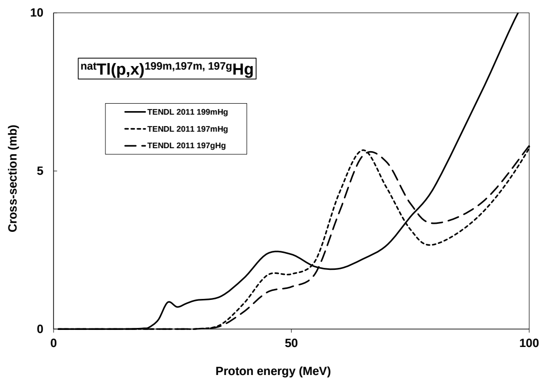

Figure 12: Activation cross-sections for production of ^{199m}Hg, ^{197m}Hg and ^{197g}Hg isomeric states predicted in TENDL 2011

$^{nat}Tl(p, xn)^{203}Hg$ reaction

The ^{203}Hg (46.594 d) is produced through the $^{205}Tl(p, 2pn)$ reaction. It has the same energy γ-line (279 keV) as the ^{203}Pb (51.92 h), therefore it was measured after complete decay of ^{203}Pb. Only a few experimental data points were measured above the effective threshold (Fig. 13).

4.2. Integral yields

From fits to our experimental excitation functions thick target physical yields (Bonardi, 1987) were calculated (no saturation effects, obtained in an irradiation time that is very short compared to the half-life of the radionuclide). The integral yields for ^{201}Pb, ^{202m}Pb, ^{200}Pb, ^{203}Pb and ^{204m}Pb (related to production of ^{201}Tl and ^{203}Pb) are shown in Figs. 14-18 in comparison with the directly measured data in the literature. Only very few experimental thick target yield data were found in the literature. The data reported for enriched and natural targets were normalized according to the real isotopic

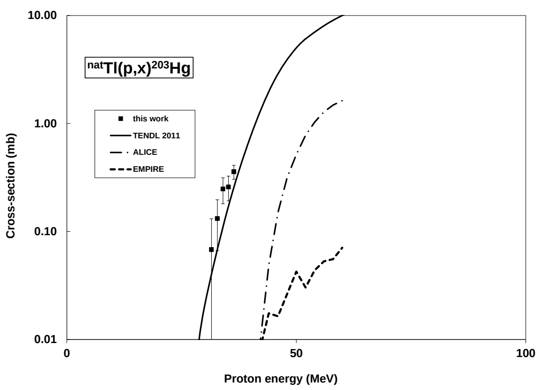

Figure 13: Excitation function of ${}^{nat}Tl(p,x)^{203}Hg$ reaction

composition and to the contributing reactions. Our calculated integral yield values for the production of ${}^{203}Pb$ and are higher than the direct yield data. In cases of ${}^{202m}Pb$ and ${}^{201}Pb$ our calculated data are surprisingly lower. No experimental thick target yield data were found for ${}^{200}Pb$ in the literature.

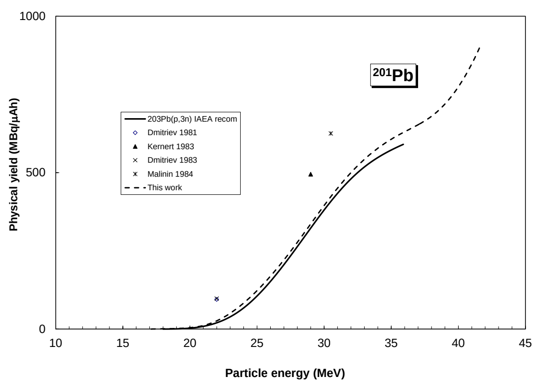

Figure 14: Integral yields of ${}^{201}Pb$ calculated from the measured excitation functions in comparison with experimental thick target yields from literature

5. Summary and conclusions

The principal aim of this investigation was remeasurement and evaluation of the cross-section data of the production of ${}^{201}Tl$.

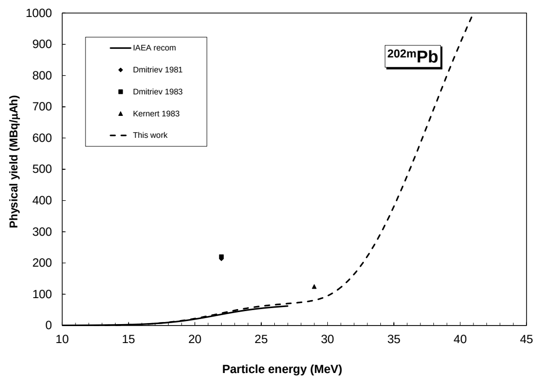

Figure 15: Integral yields of ${}^{202m}Pb$ calculated from the measured excitation functions in comparison with experimental thick target yields from literature

1. We present new excitation curves for proton induced reactions on ${}^{nat}Tl$ targets up to 42 MeV leading to the production of ${}^{204m}Pb$, ${}^{203}Pb$, ${}^{202m}Pb$, ${}^{201}Pb$, ${}^{200}Pb$, ${}^{199}Pb$, ${}^{202}Tl$ (dir, cum), ${}^{201}Tl$ (dir, cum), ${}^{200}Tl$(dir) and ${}^{203}Hg$.
2. Detailed literature search was done and the literature data were critically analyzed (the earlier errors were corrected, the derived data were changed to original experimental data).
3. To upgrade the recommended cross-section data new experimental data were involved (Hanna (Al-Saleh et al., 2007; Hanna et al., 1977), this work).
4. To check the predictivity of the theoretical codes, new theoretical calculations were done based on new versions of the model codes.

5.1. The new experimental data:

As our excitation functions are correlated to monitor reactions re-measured over the whole energy range simultaneously the uncertainties in incident energy, average energy in each foil and number of bombarding particles are diminished.

5.2. The evaluation process:

1. Except a few old works the experimental data shows surprisingly good agreement.
2. The description of the theoretical codes is acceptable good.
3. The new recommended data from point of view of production of ${}^{201}Tl$ and the ${}^{200}Tl$ and ${}^{202}Tl$ impurities didn't differ significantly from recommended data in the IAEA medical library.

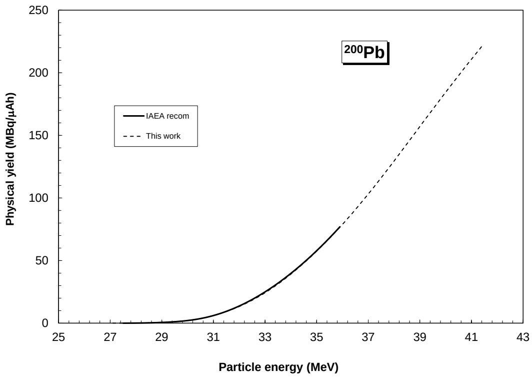

Figure 16: Integral yields of ${}^{200}Pb$ calculated from the measured excitation functions in comparison with experimental thick target yields from literature

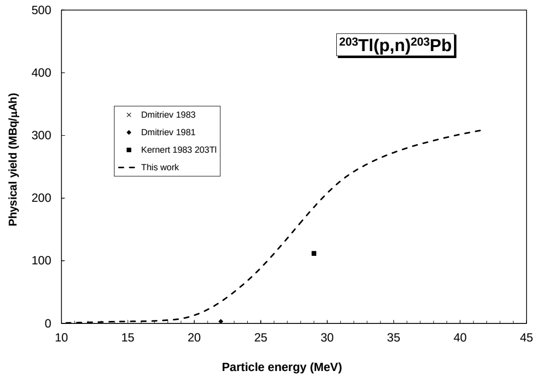

Figure 17: Integral yields of ${}^{203}Pb$ calculated from the measured excitation functions in comparison with experimental thick target yields from literature

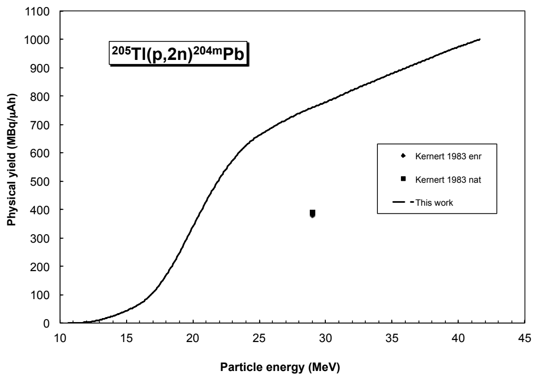

Figure 18: Integral yields of ${}^{204m}Pb$ calculated from the measured excitation functions in comparison with experimental thick target yields from literature

4. No proper thick target yield data were measured for validation of the excitation functions (low beam intensity measurements at around 30 MeV).
5. There are good review works discussing the optimization of the ${}^{201}Tl$ production and the chemical processes (Afarideh et al., 2004; Al-Saleh et al., 2007; Birattari et al., 1982; Fernandes and da Silva, 1992; Groppi et al., 2001; Haji-Saeid et al., 2009; Hanna et al., 1977; Lagunas-Solar et al., 1981, 1978; Malinin et al., 1984; Qaim et al., 1979; Sattari et al., 2003; Sheu et al., 2003)(.
6. Except excitation functions of Lagunas Solar (Lagunas-Solar et al., 1978) measured up to 60 MeV for production of ${}^{200-204}Pb$, no experimental data exists above 40 MeV

5.3. Application of the new experimental and evaluated data:

1. Optimization of the production of the medically used ${}^{201}Tl$.
2. The measured excitation functions can be used for determination of thallium in different materials by proton activation analysis (De Brucker et al., 1989; Wauters et al., 1987).
3. To estimate the radiation dose caused by proton activation of the materials with thallium content (glasses, semiconductors, particle detectors, high temperature superconductors, etc.)
4. Application of ${}^{203}Pb$ emitting imaginable γ-ray (279 keV) for bio-distribution and targeting studies of the cytotoxic alpha-emitting ${}^{212}Pb$-radiolabeled compounds and antibodies (Chappell et al., 2000; Garmestania et al., 2005) . Preparation of ${}^{203}Pb$ compounds for studies on pathway and effects of lead pollution (Girardi et al., 1975) .
5. To upgrade the nuclear reaction model codes and their input parameters.

6. Acknowledgements

This study was performed in the frame of the MTA-FWO (Vlaanderen) collaboration program. The authors thank the different research projects and their respective institutions for the practical help and providing the use of the facilities for this study. Special thanks to V. Semkova (IAEA) for valuable help in literature search.

Table 2: Summary of earlier experimental investigations on activation cross-sections and yields of the proton induced nuclear reaction on thallium (abbreviations for the measured quantities are taken from the EXFOR, see in footnote)

Author	**Target**	**Irradiation**	**Beam current measurement and monitor reaction**	**Measurement of activity and separation method**	**Nuclear reaction, measured quantity, number of measured data points**	**Covered energy range (MeV)**
Sakai, (Sakai et al., 1965)	^{nat}Tl	cyclotron stacked foil	Faraday cup	chemical separation γ-Na(I)	^{nat}Tl(p,x)^{200}Pb, s, 6 ^{nat}Tl(p,x)^{201}Pb, s, 6 ^{nat}Tl(p,x)^{203}Pb, s, 6	10.5-51.6 10.4-51.7 10.0-51.5
Lebowitz, (Lebowitz et al., 1975)	^{nat}Tl ˜0.2 mg/cm^2	cyclotron stacked foil	Faraday cup	chemical separation γ-Ge(Li)	^{203}Tl(p,3n)^{201}Pb, s, 6	19.28-32.15
Milazzo-Colli (Milazzo-Colli et al., 1975)	^{203}Tl, ^{205}Tl 300-400 μg/cm^2	cyclotron		α-Si surface barrier	^{203}Tl(p,a)^{200}Hg, s, 1 ^{205}Tl(p,a)^{202}Hg, s, 1	20 20
Dmitriev, (Dmitriev et al., 1976)	^{nat}Tl thick target	cyclotron single foil	Faraday cup	no chemical separation γ-Ge (Li)	^{203}Tl(p,np)^{202}Tl, TTY, 1 ^{203}Tl(p,3n)^{201g}Pb,TTY, 1 ^{203}Tl(p,2n)^{202m}Pb, TTY, 1 ^{nat}Tl(p,x)^{203g}Pb, TTY, 1	22 22 22 22
Hanna, (Hanna et al., 1977)	^{nat}Tl 275 mg/cm^2	cyclotron EN tandem VdG stacked foil	Faraday cup	chemical separation γ-Ge (Li)	^{nat}Tl(p,x)^{200}Pb,TTD, REL, 4 ^{nat}Tl(p,x)^{201}Pb,TTD, REL, 6 ^{nat}Tl(p,x)^{202}Tl, TTD, REL, 7	26.89-34.84 20.4-34.87 16.27-34.84
J. W. Blue, (Blue et al., 1978)	^{nat}Tl foil 110μm	cyclotron stacked foil	Faraday cup	no chemical separation γ-Ge(Li)	^{203}Tl(p,3n)^{201}Pb, s, 12 ^{203}Tl(P,4N)^{200}Pb, s, 6	18.47-35.19 27.91-35.1
Lagunas-Solar (Lagunas-Solar et al., 1978)	^{nat}Tl 0.16-0.20 g/cm^2	cyclotron stacked foil	Faraday cup	no chemical separation γ-Ge(Li)	^{nat}Tl(p,x)^{200}Pb, PY, FCT, 31 ^{203}Tl(p,x)^{200}Pb, s, DERIV, 14 ^{nat}Tl(p,x)^{201}Pb, PY, FCT, 68 ^{203}Tl(p,x)^{201g}Pb, M+, s, DERIV, 39 ^{nat}Tl(p,x)^{201}Tl, TTY, DT, 41 ^{203}Tl(p,x)^{202m}Pb, s, DERIV, 41 ^{nat}Tl(p,x)^{203}Pb, PY, FCT, 45 ^{nat}Tl(p,x)^{203}Pb, s, DERIV, 45 ^{nat}Tl(p,x)^{204m}Pb, PY, FCT, 30 ^{nat}Tl(p,x)^{204m}Pb, s, DERIV, 30 ^{205}Tl(p,x)^{200}Pb, s, DERIV, 11 ^{205}Tl(p,x)^{201g}Pb, M+, s, DERIV, 23 ^{205}Tl(p,x)^{202m}Pb, s, DERIV, 23	28.4-59.3 30.0-40.9 17.2-59.0 18.3-33.6 11.8-35.9 17.0-27.4 17.0-59.1 17.0-59.1 13.6-35.8 15.3-35. 46.8-59.3 38.2-59.0 27.4-35.9
Qaim et al. (Qaim et al., 1979)	^{nat}Tl 50-125μm	cyclotron stacked foil	^{63}Cu(p,2n)^{62}Zn ^{63}Cu(p,p2n)^{61}Cu	no chemical separation γ-Ge(Li)	^{205}Tl(p,2n)^{204m}Pb, s, 27 ^{nat}Tl(p,x)^{203}Pb, IND, s, 34 ^{nat}Tl(p,x)^{202m}Pb, IND, s, 31 ^{nat}Tl(p,x)^{201}Pb, IND, s, 25 ^{nat}Tl(p,x)^{200}Pb, IND, s, 14 ^{nat}Tl(p,x)^{199}Pb, IND, s, 5 ^{nat}Tl(p,x)^{202}Tl, IND, 18 ^{nat}Tl(p,x)^{201}Tl, IND, s, 11	12.1-44.2 7.49-44.4 9.59-44.2 17.2-44.1 28.2-44.4 38.6-44.3 16.2-44.2 19.8-42.8
Bonardi (Bonardi et al., 1982)	^{nat}Tl foil	cyclotron stacked foil	Faraday cup	γ-Ge(Li)	^{nat}Tl(p,x)^{200}Pb, TTD, 7 ^{nat}Tl(p,x)^{201}Pb, TTD, TM, 12 ^{nat}Tl(p,x)^{202}Tl, TTD, TTY, TM, 13 ^{nat}Tl(p,x)^{203}Pb, TTD, TTY, TM, 17 ^{203}Tl(p,x)^{200}Pb, TTD, 6 ^{203}Tl(p,x)^{201}Pb, TTD, 11 ^{203}Tl(p,x)^{202m}Pb, TTD, 14 ^{203}Tl(p,x)^{203}Pb, TTD, 14	27.696-42.24 18.823-42.067 16.677-42.143 7.3794-42.177 28.234-36.021 20.755-35.984 14.015-36.023 14.001-35.983
Kernert (Kernert et al., 1983)	^{203}Tl (99%) ^{nat}Tl thick target	cyclotron single target	Faraday cup		^{203}Tl(p,x)^{201}Pb, TTY, 1 ^{203}Tl(p,x)^{202m}Pb, TTY, 1 ^{203}Tl(p,x)^{203}Pb, TTY, 1 ^{203}Tl(p,x)^{204m}Pb, TTY, 1 ^{nat}Tl(p,x)^{201}Pb, TTY, 1 ^{nat}Tl(p,x)^{202m}Pb, TTY, 1 ^{nat}Tl(p,x)^{203}Pb, TTY, 1 ^{nat}Tl(p,x)^{204m}Pb, TTY, 1	29 29 29 29 29 29 29 29
Malinin (Malinin et al., 1984)	^{203}Tl (96.9%) 0.35-0.4 g/cm^2	cyclotron single target	Faraday cup	chemical separation γ-Ge(Li)	^{203}Tl(p,x)^{201}Pb, TTY, 1	30.5
Hermanne (Hermanne et al., 1992)	^{nat}Tl (50μ m)	cyclotron stacked foil	Faraday cup	no chemical separation γ-Ge(Li)	^{203}Tl(p,2n)^{202m}Pb, s, DERIV, 13 ^{203}Tl(p,3n)^{201}Pb, s, DERIV, 22 ^{203}Tl(P,4N)^{200}Pb, s, DERIV, 12 ^{205}Tl(p,2n)^{204m}Pb, s, DERIV, 29 ^{203}Tl(p,3n)^{203}Pb, s, DERIV, 24 ^{203}Tl(p,4n)^{202m}Pb, s, DERIV, 12 ^{203}Tl(p,2n)^{201}Pb, s, DERIV, 4	15-27 19-42 29-42 12-42 17-40 29-40 38-42
Sattari (Sattari et al., 2003)	^{203}Tl(enr.) 18.3 μ m	cyclotron single target	Faraday cup	γ-HpGe(Li)	^{203}Tl(p,x)^{201}Pb, TTY, REL, 4	28-30
Al-Saleh (Al-Saleh et al., 2007)	^{nat}Tl 10-15μ m thick on 10μ m Cu	cyclotron stacked foil	Faraday cup ^{29}Cu(p,x)^{63}Zn monitor	no chemical separation g-HpGe	^{nat}Tl(p,x)^{201}Pb, s = ^{203}Tl(p,3n)^{201}Pb, s, 17 ^{nat}Tl(p,x)^{202m}Pb, s = ^{203}Tl(p,2n)^{202m}Pb, s + ^{205}Tl(p,4n)^{202m}Pb, s, 23 ^{nat}Tl(p,x)^{203}Pb, s = ^{203}Tl(p,n)^{203}Pb, s + ^{205}Tl(p,3n)^{203}Pb, s, 34	19.3-27.2 15.7-27.2 6.2-27.2
					^{nat}Tl(p,x)^{204m}Pb, s = ^{205}Tl(p,2n)^{204m}Pb, s, 28	11.3-27.2
this work Ser. 1	^{nat}Tl (50μ m) on Cu (50μ m)	cyclotron stacked foil	Faraday cup	no chemical separation γ-Ge(Li)	^{nat}Tl(p,x)^{204m}Pb, 105 ^{nat}Tl(p,x)^{203}Pb, 73 ^{nat}Tl(p,x)^{202m}Pb, N110 ^{nat}Tl(p,x)^{201}Pb, 81 ^{nat}Tl(p,x)^{200}Pb, 67 ^{nat}Tl(p,x)^{199}Pb, 17	12.2-41.7 10.8-41.7 10.8-41.7 17.1-41.7
this work Ser. 2	^{nat}Tl (20.8 μ m) on Cu (12.5 μ m)	cyclotron	Faraday cup ^{nat}Cu(p,x)^{62,65}Zn	no chemical separation γ-HpGe	^{nat}Tl(p,x)^{204m}Pb, 20 ^{nat}Tl(p,x)^{203}Pb, 20 ^{nat}Tl(p,x)^{202m}Pb, 20 ^{nat}Tl(p,x)^{201}Pb, 20 ^{nat}Tl(p,x)^{200}Pb, 20 ^{nat}Tl(p,x)^{202}Tl, 20 ^{nat}Tl(p,x)^{201}Tl, 20 ^{nat}Tl(p,x)^{200}Tl, 20 ^{nat}Tl(p,x)^{203}Hg, 20	27.1-41.5

SIG-Cross section, TTY-thick target yield, TTD-differential thick target yield, DERIV-derived data, IND-independent formation, CUM-cumulative formation, REL-relative

Table 3: The most important compilations and theoretical calculations on cross-sections and yields of ^{nat}Tl(p,x)^{201}Pb?^{201}Tl and the side reactions

Author	Model code	Reactions	Compilation	Recommended
Canedrias Ruz (Canderias-Cruz and Okamoto, 1987)		^{nat}Tl(p,x)^{201}Pb	X	
Rurarz (Rurarz, 1994)		^{nat}Tl(p,x)^{201}Pb	X	
Kurenkov (Kurenkov et al., 1995)	ALICE-87, STAPRE	^{203,205}Tl(p,xn)		
IAEA TECDOC (Hermanne et al., 2001)	ALICE-IPPE, ALICE-HMS	^{nat}Tl(p,x)^{201}Pb ^{nat}Tl(p,x)^{202}Pb ^{nat}Tl(p,x)^{200}Pb	X	X
Takcs (Takcs et al., 2005)		^{nat}Tl(p,x)^{201}Pb ^{nat}Tl(p,x)^{202}Pb ^{nat}Tl(p,x)^{200}Pb	X	X
Tel (Tel et al., 2011)	ALICE/ASH	^{nat}Tl(p,x)^{201}Pb		
Haji Said (Haji-Saeid et al., 2009)		^{nat}Tl(p,x)^{201}Pb	X	
Sheu (Sheu et al., 2003)	ALICE-01, Fluka	^{nat}Tl(p,x)^{201}Pb	X	
Landolt Bornstein (Iljinov et al., 1993)		^{nat}Tl(p,x)^{201}Pb ^{nat}Tl(p,x)^{202}Pb ^{nat}Tl(p,x)^{200}Pb	X	
Mihilescu (Mihilescu et al., 2007)				
Lagunas-Solar (Lagunas-Solar et al., 1978)	STAPRE			
Groppi (Groppi et al., 2001)		^{nat}Tl(p,x)^{201}Pb	X	
Shubin (Shubin, 2001)				
Nowotny (Nowotny, 1981)				
MENDL -2P (Shubin et al., 1998)	ALICE-IPPE	^{nat}Tl(p,x)^{201}Pb ^{nat}Tl(p,x)^{202}Pb ^{nat}Tl(p,x)^{200}Pb		
Koning (Koning and Rochman, 2011)	TALYS	^{nat}Tl(p,x)^{201}Pb ^{nat}Tl(p,x)^{202}Pb ^{nat}Tl(p,x)^{200}Pb		
Szelecsényi (Szelecsényi et al., 1995)				
Dmitriev (Dmitriev and Zaitseva, 1996)			X	
Kaplan (Kaplan et al., 2009)	CEM cascade-exciton model GDH model Hybrid model Equilibrium model	^{203}Tl(p,n)^{203}Pb ^{203}Tl(p,2n)^{202}Pb ^{203}Tl(p,3n)^{201}Pb ^{203}Tl(p,4n)^{200}Pb ^{205}Tl(p,3n)^{203}Pb ^{205}Tl(p,4n)^{202}Pb ^{205}Tl(p,5n)^{201}Pb ^{205}Tl(p,6n)^{200}Pb		

Table 4: Comparison of the γ-ray intensities used by different authors

Nuclide J^p level energy (MeV)	**Half-life**	**E_γ(keV) NUDAT**	**I_γ (%) NUDAT**	**I_γ(%) Lag-Sol**	**I_γ (%) Qaim**	**I_γ (%) Al Saleh**	**I_γ (%) Bonardi**	**I_γ (%) Dmitriev**	**I_γ (%) Hermanne 1991**
^{204m}Pb 9- 2185.88	66.93 m	374.76 899.15 911.74	94.20 99.174 91.5	99.2	95 100 100	89 99			94.2 99.3
^{203}Pb 5/2-	51.92 h	279.1952 401.320	80.9 3.35	81.0	80.7	99 90.7	80.8 3.35	81 3.8	80 3.8
^{202m}Pb 9- 2169.83	3.54 h	422.12 657.49 786.99 960.70 389.94 459.72 490.47	84 31.7 49 89.9 6.6 9.2 9.8	85.3	90 56 89	96 50	85.66 32.4 49.8 91.3		86 35 50 89
^{201}Pb 5/2-$^+$	9.33 h	331.15 361.25 405.96 584.60 692.41 767.26 826.26 907.67 945.96	77 9.5 2.03 3.6 4.3 3.28 2.38 6.1 7.2	61.4	82 10.7	79 9.9	3.56 4.27 5.70 7.36		82 10.7
^{200}Pb 0+	21.5 h	147.63 235.62 257.19 268.36 450.56	38.2 4.35 4.52 4.01 3.37	28.4	30.8		37.73 4.3 4.46 3.96		29
^{199}Pb 3/2-	90 m	366.90 720.24 1135.04	44 % 6.5 7.8		11.6 14				79 11.4
^{202}Tl 2-	12.31 d	439.510	91.5		95	91.4			
^{201}Tl 1/2+	3.0421 d	135.34 167.43	2.565 10.00		2.65	2.565			
^{200}Tl 2-	26.1 h	367.942 579.300 828.27 1205.75	87 13.7 10.8 30			87.2 13.78 10.81 29.91			
^{203}Hg 5/2-	46.594 d	279.1952	81.56						

Table 5: Nuclear data of the investigated reactions for ^{nat}Tl+ p

Nuclide **J^p** **level energy (MeV)**	**Half-life**	**Decay mode (%)**	**E$_\gamma$ (keV)**	**I$_\gamma$ (%)**	**Contributing reactions**	**Q-value (keV)**
^{204m}Pb 9- 2185.88	66.93 m	IT(100)	374.76 899.15 911.74	94.20 99.174 91.5	^{203}Tl(p,g) ^{205}Tl(p,2n)	6637.51 -7564.517
^{203}Pb 5/2-	51.92 h	EC(100)	279.1952 401.320	80.9 3.35	^{203}Tl(p,n) ^{205}Tl(p,3n)	-1756.97 -15959.0
^{202m}Pb 9- 2169.83	3.54 h	IT(90.5) EC(9.5)	422.12 657.49 786.99 960.70 389.94 459.72 490.47	84 31.7 49 89.9 6.6 9.2 9.8	^{203}Tl(p,2n) ^{205}Tl(p,4n)	-8681.26 -22883.29
^{201}Pb 5/2-$^+$	9.33 h	EC(100)	331.15 361.25 405.96 584.60 692.41 767.26 826.26 907.67 945.96	77 9.5 2.03 3.6 4.3 3.28 2.38 6.1 7.2	^{203}Tl(p,3n) ^{205}Tl(p,5n)	-17428.3 -31630.3
^{200}Pb 0+	21.5 h	EC(100)	147.63 235.62 257.19 268.36 450.56	38.2 4.35 4.52 4.01 3.37	^{203}Tl(p,4n) ^{205}Tl(p,6n)	24514.2 -38716.2
^{199}Pb 3/2-	90 m	EC(100)	366.90 720.24 1135.04	44 % 6.5 7.8	^{203}Tl(p,5n) ^{205}Tl(p,7n)	-33600.8 -47802.9
^{202}Tl 2-	12.31 d	EC(100)	439.510	91.5	^{203}Tl(p,pn) ^{205}Tl(p,p3n) ^{202m}Pb decay	-7849.2 -22051.3
^{201}Tl 1/2+	3.0421 d	EC(100)	135.34 167.43	2.565 10.00	^{203}Tl(p,p2n) ^{205}Tl(p,p4n) ^{201}Pb decay	-14721.8 -28923.8
^{200}Tl 2-	26.1 h	EC(100)	367.942 579.300 828.27 1205.75	87 13.7 10.8 30	^{203}Tl(p,p3n) ^{205}Tl(p,p5n)	-22927.04 -37129.08
^{203}Hg 5/2-	46.594 d	β^-(100)	279.1952	81.56	^{205}Tl(p,2pn)	-13911.76

Abundances (%): ^{203}Tl (29.524), ^{205}Tl (70.476) Increase Q-values if compound particles are emitted: np-d, +2.2 MeV; 2np-t, +8.48 MeV; n2p-^{3}He, +7.72 MeV; 2n2p-α, +28.30 MeV Decrease Q-values for isomeric states with level energy of the isomer

Table 6: Measured cross-sections of the ^{204m}Pb,^{203}Pb,^{202m}Pb, ^{201}Pb and ^{199}Pb reactions (ser. 1). Different cross-sections by the same energy come from different stack/irradiation

E ± ΔE(MeV)		**Cross-sections (σ) ± Δσ (mb)**											
		^{204m}Pb		^{203}Pb		^{202m}Pb		^{201}Pb		^{200}Pb		^{199}Pb	
10.8	2.5			41.5	4.6	1.3	0.15						
12.2	2.4	6.6	0.7	29.9	3.3	0.8	0.09						
12.8	2.3	18.5	2.0	47.3	5.2	2.5	0.27						
14.0	2.2	20.0	2.2	25.0	2.8	2.0	0.22						
15.7	2.1	20.2	2.2	9.8	1.1	2.9	0.32						
17.1	2.0	69.9	7.7	64.2	7.1	12.8	1.41						
17.3	2.0	67.9	7.5			11.8	1.30	12.2	1.34				
18.6	1.9	88.9	9.8	92.1	10.1	18.1	1.99						
18.7	1.9					12.6	1.39						
19.9	1.8	93.3	10.3	300.6	33.1	25.1	2.76						
20.0	1.8	99.5	10.9			24.9	2.74						
20.1	1.8	99.9	11.0			24.3	2.67						
21.2	1.7	69.7	7.7	446.7	49.1	20.7	2.27	32.1	3.53				
21.3	1.7	88.4	9.7	514.1	56.6	29.6	3.26	101.7	11.18				
21.4	1.7	84.4	9.3			27.9	3.06	109.1	12.00				
21.8	1.7	77.3	8.5			27.3	3.00	104.6	11.51				
21.9	1.7	85.9	9.5	621.6	68.4	31.5	3.46	146.6	16.12				
22.5	1.6	56.7	6.2	633.7	69.7	23.6	2.59						
22.6	1.6	60.6	6.7	685.3	75.4	26.0	2.86	189.3	20.83				
23.0	1.6	71.0	7.8			30.7	3.38	202.7	22.29				
23.1	1.6	52.9	5.8	662.0	72.8	22.6	2.49						
23.1	1.6	59.8	6.6	776.6	85.4	27.0	2.97	247.2	27.19				
23.7	1.6	35.5	3.9	680.1	74.8	16.6	1.83						
23.8	1.6	40.7	4.5			20.4	2.24						
23.9	1.5	40.1	4.4	667.1	73.4	18.9	2.08	261.3	28.74				
24.2	1.5	45.6	5.0			22.4	2.47	257.9	28.37				
24.3	1.5	39.2	4.3	805.9	88.6	18.7	2.06						
24.3	1.5	41.1	4.5	897.7	98.7	21.6	2.37						
24.9	1.5	27.3	3.0	809.5	89.0	14.1	1.55	325.0	35.75				
24.9	1.5	29.8	3.3	871.3	95.8	15.0	1.65	331.8	36.50				
25.1	1.5	23.2	2.6			12.5	1.38						
25.4	1.4	22.9	2.5			11.7	1.28						
25.5	1.4	28.0	3.1	923.7	101.6	14.5	1.59	312.2	34.35				
26.0	1.4	19.8	2.2			9.5	1.04	364.9	40.14				
26.1	1.4	20.3	2.2			10.5	1.16	316.1	34.77				
26.5	1.4	22.1	2.4			10.0	1.10	345.2	37.97				
26.6	1.4	21.3	2.3	964.0	106.0	11.4	1.25	366.5	40.32				
26.7	1.3	24.5	2.7	953.1	104.8	10.9	1.20	400.2	44.02				
27.1	1.3	17.6	1.9			8.7	0.96	417.3	45.90	5.5	0.61		
27.2	1.3	19.0	2.1	889.3	97.8	8.9	0.98			1.8	0.20		
27.6	1.3	20.4	2.2	882.2	97.0	10.4	1.15	375.9	41.34	1.9	0.21		
27.6	1.3	18.0	2.0	972.9	107.0	12.4	1.36	406.3	44.70	2.2	0.25		
27.7	1.3	18.1	2.0	953.8	104.9	10.4	1.15	427.3	47.00	1.6	0.18		
27.9	1.3			972.0	106.9	12.8	1.41	408.4	44.93	2.8	0.30		
28.2	1.2	15.4	1.7			10.4	1.15	427.6	47.03	2.2	0.24		
28.2	1.2	16.3	1.8			11.3	1.24			5.5	0.60		
28.7	1.2	16.7	1.8	931.7	102.5	17.8	1.96			8.5	0.94		
28.7	1.2	16.1	1.8	849.0	93.4	20.3	2.24			9.2	1.02		
28.7	1.2	15.5	1.7			17.5	1.92	441.7	48.59	9.0	0.99		
28.9	1.2			859.7	94.6	21.6	2.38	402.9	44.32	15.2	1.67		
29.0	1.2					21.6	2.37	403.2	44.35	11.7	1.28		
29.2	1.2	13.7	1.5			21.2	2.33	411.6	45.27	11.0	1.21		
29.3	1.2	15.3	1.7			23.5	2.59			14.1	1.55		
29.7	1.1	14.7	1.6	768.2	84.5	39.4	4.33			29.5	3.25		
29.7	1.1	15.1	1.7			40.4	4.45	382.4	42.06	29.6	3.26		
29.8	1.1	10.5	1.2	792.3	87.2	41.9	4.61	406.0	44.66	30.8	3.38		
29.9	1.1	17.6	1.9	741.1	81.5	44.4	4.88	425.7	46.83	31.7	3.48		
30.0	1.1			737.4	81.1			419.9	46.19	25.2	2.77		
30.2	1.1	16.5	1.8	720.6	79.3	54.0	5.94	393.0	43.23	44.7	4.92		
30.2	1.1	14.3	1.6			46.8	5.15	407.3	44.80	39.2	4.31		
30.3	1.1	13.8	1.5			48.0	5.28			37.0	4.06		
30.6	1.1	14.9	1.6			70.2	7.72	379.4	41.73	62.7	6.90		
30.7	1.1	18.0	2.0	684.7	75.3	74.1	8.15			65.4	7.19		
30.8	1.1	15.0	1.7			71.9	7.91	404.8	44.53	66.4	7.30		
30.9	1.1	16.7	1.8			75.0	8.25	375.0	41.25	72.1	7.93		
31.0	1.1	16.5	1.8	704.3	77.5	85.4	9.39	369.2	40.61	71.8	7.90		
31.6	1.0	16.0	1.8	499.1	54.9	108.1	11.89			116.7	12.83		
31.7	1.0	15.4	1.7	468.9	51.6	108.8	11.97	323.1	35.54	114.9	12.63		
31.7	1.0	15.3	1.7	483.9	53.2	101.1	11.12	311.4	34.25	100.1	11.01		
31.8	1.0	15.0	1.7	438.6	48.2	105.7	11.62	313.5	34.48	115.3	12.68		
31.9	1.0	14.1	1.6			110.0	12.10	299.6	32.96	106.4	11.70		
32.0	1.0	14.5	1.6	399.6	44.0	96.1	10.57	325.4	35.80	105.2	11.57		
32.6	0.9	14.2	1.6	396.6	43.6	139.3	15.33	273.5	30.08	153.3	16.86		
32.9	0.9	13.6	1.5	389.7	42.9	142.7	15.70	271.3	29.84	149.9	16.48		
33.0	0.9	12.8	1.4	326.7	35.9	128.7	14.16	266.8	29.35	156.3	17.20		
33.6	0.9	14.8	1.6	325.7	35.8	174.1	19.15	233.2	25.65	203.7	22.40		
33.8	0.9	14.5	1.6	316.4	34.8	179.3	19.72	224.8	24.73	198.3	21.81		
33.9	0.8	12.9	1.4	299.7	33.0	152.7	16.79	216.9	23.85	193.5	21.28		
33.9	0.8	13.7	1.5			180.2	19.82	210.7	23.18	224.0	24.64		
34.6	0.8	13.4	1.5			190.4	20.95			234.7	25.82		
34.7	0.8	11.9	1.3	243.3	26.8	193.7	21.31	176.1	19.37	227.9	25.07		
34.8	0.8	14.6	1.6	237.6	26.1	189.8	20.88	166.9	18.36	251.0	27.61		
34.8	0.8	14.9	1.6	263.5	29.0	218.2	24.00	165.5	18.20	283.4	31.17		
35.5	0.7	14.7	1.6	208.2	22.9	227.3	25.00	180.0	19.80	281.7	30.99		
35.6	0.7	10.4	1.2	206.4	22.7	209.3	23.02	155.8	17.14	249.7	27.46		
35.7	0.7	13.4	1.5	232.3	25.6	192.9	21.22	137.7	15.15	260.6	28.66		
35.7	0.7	13.8	1.5			241.4	26.56	128.6	14.15	320.4	35.25		
36.3	0.7	13.2	1.5			236.9	26.06			304.3	33.47		
36.3	0.7	13.8	1.5	202.4	22.3	233.8	25.72	137.9	15.17	291.6	32.07		
36.4	0.7	12.9	1.4	193.2	21.3	222.5	24.47	136.6	15.03	283.1	31.14		
36.4	0.7	9.2	1.0	188.2	20.7	222.9	24.52	129.3	14.22	271.1	29.82		
36.6	0.7	12.9	1.4	185.0	20.4	204.6	22.50	126.8	13.95	273.8	30.12		
36.6	0.7	12.5	1.4			240.5	26.45	118.6	13.04	309.8	34.08	2.2	0.2
36.9	0.6	12.3	1.4			198.0	21.78	143.5	15.78				
37.4	0.6	10.5	1.2			215.9	23.75	121.7	13.38	293.5	32.28		
37.4	0.6	11.1	1.2	149.8	16.5	227.6	25.04	148.6	16.35	301.7	33.19	2.5	0.3
37.8	0.6	12.7	1.4	162.6	17.9	216.0	23.76	154.3	16.98				
38.3	0.5	11.7	1.3	154.3	17.0	252.4	27.76	137.6	15.14	343.3	37.76	12.9	1.4
38.3	0.5	13.4	1.5	167.0	18.4	261.6	28.77	225.1	24.76	357.8	39.35	9.8	1.1
38.5	0.5	12.3	1.4			223.9	24.63	236.8	26.05			15.4	1.7
39.1	0.5	11.6	1.3	149.3	16.4	244.2	26.86	223.8	24.62	328.5	36.13	22.6	2.5
39.1	0.5	11.4	1.3	131.1	14.4	218.4	24.02	295.7	32.53	304.2	33.46	20.5	2.3
39.3	0.5	10.5	1.2	128.9	14.2	206.3	22.69	259.5	28.54			30.1	3.3
39.9	0.4	12.5	1.4	127.9	14.1	198.7	21.86	275.0	30.25	294.7	32.42	34.2	3.8
39.9	0.4	10.6	1.2					321.4	35.35	290.4	31.95	41.5	4.6 2
40.1	0.4	9.3	1.0			172.8	19.01					46.4	5.1
40.7	0.4	10.0	1.1			203.9	22.43	314.4	34.58	302.5	33.27	66.5	7.3
40.7	0.4	10.4	1.2	120.4	13.3	185.8	20.44	449.0	49.38	283.8	31.22	63.2	7.0
40.9	0.4	8.6	0.9	98.9	10.9	160.1	17.61	436.9	48.05			70.6	7.8
41.5	0.3	11.0	1.2	111.1	12.2	180.5	19.85			274.6	30.20	91.5	10.1
41.5	0.3	10.3	1.1	116.8	12.9	179.3	19.72			275.2	30.27	98.9	10.9
41.7	0.3	9.4	1.0	105.3	11.6	157.8	17.35	515.5	41.24			93.8	10.3

Table 7: Measured cross-sections of the ^{204m}Pb,^{203}Pb,^{202m}Pb, ^{201}Pb, and ^{200}Pb reactions (ser. 2)

E ± ΔE(MeV)		**Cross-sections (σ) ± $\Delta\sigma$ (mb)**									
		^{204m}Pb		^{203}Pb		^{202m}Pb		^{201}Pb		^{200}Pb	
36.4	0.3	11.4	1.4	204.2	23.0	227.2	24.6	113.1	12.7	270.7	29.3
35.2	0.3	11.5	1.3	232.6	26.0	197.7	21.4	130.8	14.3	251.0	27.2
34.0	0.3	13.6	1.5	275.8	30.5	176.2	19.1	166.6	18.1	206.1	22.3
32.8	0.3	12.6	1.4	362.0	40.3	137.3	14.9	217.5	23.6	211.1	22.9
31.5	0.4	14.3	1.6	468.1	51.0	103.6	11.2	275.5	29.9	88.5	9.6
30.2	0.4	14.7	1.6	621.7	67.8	59.3	6.5	316.1	34.3	44.1	4.8
28.8	0.4	16.8	1.9	769.6	83.7	26.4	2.9	355.0	38.5	11.7	1.4
27.4	0.5	18.8	2.6	836.4	90.9	10.2	1.2	345.7	37.6	0.5	0.5
25.9	0.5	22.5	2.7	858.9	93.4	11.8	1.4	338.7	37.0		
24.4	0.6	28.0	3.1	768.7	83.5	17.0	1.9	287.3	31.3		
22.8	0.6	45.7	5.2	686.2	74.7	26.6	2.9	223.7	24.3		
21.1	0.7	73.7	8.2	532.2	58.0	31.0	3.4	127.8	14.0		
19.3	0.8	96.2	10.8	244.2	26.8	28.6	3.2	22.8	3.5		
17.8	0.9	75.8	8.2	65.1	8.2	25.7	2.8				
16.2	0.9	63.4	6.9	11.1	3.4	12.8	1.4				
14.6	1.0	33.4	3.6	20.3	2.9	10.4	1.2				
12.7	1.1	11.8	1.5	36.5	4.2						
10.6	1.3	0.6	0.3	40.2	4.5						
9.3	1.4			27.8	3.3						
7.9	1.5			10.1	1.1						

Table 8: Measured cross-sections of the ^{202}Tl, ^{201}Tl, ^{200}Tl, and ^{203}Hg reactions (ser.2)

E ± ΔE(MeV)		**Cross-sections (σ) ± $\Delta\sigma$ (mb)**							
		^{202}Tl		^{201}Tl		^{200}Tl		^{203}Hg	
36.4	0.3	80.1	8.9	54.8	23.8	5.1	0.6	0.36	0.05
35.2	0.3	77.8	8.7			2.5	0.3	0.26	0.07
34.0	0.3	67.6	7.6	51.8	28.4	2.9	0.3	0.25	0.07
32.8	0.3	64.8	7.3			1.5	0.2	0.13	0.07
31.5	0.4	58.4	6.4	85.3	27.1	1.5	0.2	0.07	0.06
30.2	0.4	46.6	5.4	79.9	27.0	0.6	0.1		
28.8	0.4	46.0	5.3	99.6	29.9				
27.4	0.5	41.7	4.8	149.5	28.9				
25.9	0.5	33.7	4.0	98.9	23.9				
24.4	0.6	30.8	3.6	72.0	23.9				
22.8	0.6	26.4	3.2	112.8	29.2				
21.1	0.7	20.5	2.6	38.6	11.8				
19.3	0.8	14.6	1.8	1.0	8.7				
17.8	0.9	10.3	1.3						
16.2	0.9	5.4	0.8						
14.6	1.0	2.2	0.3						
12.7	1.1	0.8	0.2						
10.6	1.3								
9.3	1.4	0.3	0.1						
7.9	1.5	0.4	0.1						

References

Adam-Rebeles, R., Hermanne, A., Van den Winkel, P., Tárkányi, F., Takács, S., 2011. Activation cross section of deuteron induced reactions on natural thallium for the production of 203pb. Journal of the Korean Physical Society 59, 1975–1978.

Adam-Rebeles, R., Van den Winkel, P., Hermanne, A., Tárkányi, F., Takács, S., 2012. Experimental excitation functions of deuteron induced reactions onnatural thallium up to 50 mev. Nuclear Instruments & Methods in Physics Research Section B (accepted).

Afarideh, H., Al-Jammaz, I., Arzumanov, A., Casale, G., Dudu, D., Haji-Saeid, M., Narasimhan, D. V. S., Schlyer, D., Solin, L., Takcs, S., Van den Winkel, P. N., Vera Ruiz, H., Zhou, W., 2004. Standardized high current solid targets dor cyclotron production of diagnostic and therapeutic radionuclides. Tech. rep., IAEA.

Al-Saleh, F. S., Al-Harbi, A. A., Azzam, A., 2007. Yield and excitation function measurements of some nuclear reactions on natural thallium induced by protons leading to the production of medical radioisotopes 201tl and 203pb. Radiochimica Acta 95 (3), 127–132.

Andersen, H. H., Ziegler, J. F., 1977. Hydrogen stopping powers and ranges in all elements. The Stopping and ranges of ions in matter, Volume 3. The Stopping and ranges of ions in matter. Pergamon Press, New York.

Bell, E., Skarsgard, H. M., 1956. Cross sections of (p, xn) reactions in the isotope of lead and bismuth. Canadian Journal of Physics 34 (8), 745–766.

Birattari, C., Bonardi, M., Salomone, A., 1982. Tl-201 production studies by tl-203 (p,3n) pb-201 and hg-202 (p,2n) nuclear-reactions. Journal of Labelled Compounds & Radiopharmaceuticals 19 (11-1), 1330–1332.

Blue, J. W., Liu, D. C., Smathers, J. B., 1978. Thallium-201 production with the idle beam from neutron therapy. Medical Physics 5 (6), 532–5.

Bonardi, M., 1987. The contribution to nuclear data for biomedical radioisotope production from the milan cyclotron facility.

Bonardi, M., Birattari, C., Salomone, A., 1982. 201-tl production for medical use by (p,xn) nuclear reactions on tl and hg natural and enriched targets. In: Conf.on Nucl.Data for Sci.and Technol. p. 916.

Browne, E., Firestone, R. B., 1986. Table of Radioactive Isotopes. John Wiley & Sons, New York.

Canderias-Cruz, D., Okamoto, J., 1987. Nuclear data for medical radioisotopes produced by accelerators-status and compilation. In: IAEA Consultants Meeting on Data Requirements for Medical Radioisotope Production. pp. INDC(NDS)–195–GZ, 1998, p.145.

Chappell, L. L., Dadachova, E., Milenic, D. E., Garmestani, K., Wu, C. C., Brechbiel, M. W., 2000. Synthesis, characterization, and evaluation of a novel bifunctional chelating agent for the lead isotopes pb-203 and pb-212. Nuclear Medicine and Biology 27 (1), 93–100.

Comar, D., Crouzel, C., 1975. Preparation of carrier-free radioactive thallium for medical use. Radiochemical and Radioanalytical Letters 23 (3), 131–137.

De Brucker, N., Dewaele, J., Strijckmans, K., Vandecasteele, C., 1989. Determination of thallium in zinc by proton activation-analysis. Analytica Chimica Acta 220 (1), 93–102.

Dityuk, A. I., Konobeyev, A. Y., Lunev, V. P., Shubin, Y. N., 1998. New version of the advanced computer code alice-ippe. Tech. rep., IAEA.

Dmitriev, P. P., Molin, G. A., Dmitrieva, Z. P., Panarin, M. V., 1976. Yields of tl-200, tl-201, tl-202, and tl-204 during proton and deuteron irradiation of mercury. Soviet Atomic Energy 41 (6), 1091–1093.

Dmitriev, S. N., Zaitseva, N. G., 1996. Radionuclides for biomedical studies. nuclear data and production methods in charged-particle accelerators. Physics of Particles and Nuclei 27 (4), 403–427.

Erdtmann, G., Soyka, W., 1979. The Gamma Rays of the Radionuclides. Verlag Chemie, Weinheim, New-York.

Fernandes, L., da Silva, C. P. G., 1992. A study of irradiation conditions of mercury target with protons to obtain thallium-201. Journal of Labelled Compounds and Radiopharmaceuticals 31 (12), 967–971.

Garmestania, K., Milenica, D. E., Bradya, E. D., Plascjakb, P. S., Brechbiela, M. W., 2005. Purification of cyclotron-produced 203pb for labeling herceptin. Nuclear Medicine and Biology 32 (3), 301–305.

Girardi, F., Goetz, L., Sabbioni, E., Marafante, E., Merlini, M., Acerbi, E., Birattari, C., Castiglioni, M., Resmini, F., 1975. Preparation of pb-203 compounds for studies on pathway and effects of lead pollution. International Journal of Applied Radiation and Isotopes 26 (5), 267–277.

Gloris, M., Michel, R., Sudbrock, F., Herpers, U., Malmborg, P., Holmqvist, B., 2001. Proton-induced production of residual radionuclides in lead at intermediate energies. Nuclear Instruments & Methods in Physics Research Section a-Accelerators Spectrometers Detectors and Associated Equipment 463 (3), 593–633.

Groppi, F., Bonardi, M., Birattari, C., Gini, L., Severgnini, M., Mainardi, C., 2001. A rapid improved method for gamma-spectrometry determination of thallium-202 impurities in [thallium-201] labeled radiopharmaceuticals. Tech. rep., Istituto Nazionale di Fisica Nucleare.

Haji-Saeid, M., Pilai, M. R. A., Ruth, T. J., Schleyer, D. J., Van den Winkel, P., Vora, M. M., Capote-Noy, R., Carroll, L., Clark, J. C., Comor, J., Dehnel, M., Ferrieri, R., Finn, R. D., Fowler, J. S., Schueller, M. J., Trknyi, F., 2009. Cyclotron produced radionuclieds: Physical characteristics and production methods. Tech. rep., IAEA.

Hanna, R. W., Leigh, J. R., Burch, W. M., 1977. Production and separation of tl-201 suitable for clinical myocardial imaging. Australasian Radiology 21 (4), 387–393.

Herman, M., Capote, R., Carlson, B. V., Oblozinsky, P., Sin, M., Trkov, A., Wienke, H., Zerkin, V., 2007. Empire: Nuclear reaction model code system for data evaluation. Nuclear Data Sheets 108 (12), 2655–2715.

Hermanne, A., Gul, K., Mustafa, M. G., Nortier, M., Oblozinsky, P., Qaim, S. M., Scholten, B., Shubin, Y. N., Tárk'anyi, F., Tak'acs, S., Youxiang, Z., 2001. Production cross-sections for diagnostic radioisotopes (chapter 5). gamma emitters (5.1). Tech. rep., IAEA.

Hermanne, A., Walravens, N., Cichelli, O., 1992. Optimisation of isotope production by cross section determination. In: Qaim, S. M. (Ed.), International conference on nuclear data for science and technology. Springer, pp. 616–618.

Iljinov, A. S., Semenov, V. G., Semenova, M. P., Sobolevsky, N. M., Udovenko, L. V., 1993. Production of Radionuclides at Intermediate Energies Interactions of Protons with Targets from I to Am. Vol. 13. Springer, Berlin-Heidelberg-New York.

Janni, J. F., 1966. Calculations of energy loss, range, path length, straggling, multiple scattering and the probability of inelastic nuclear collisions for 0.1 to 1000 mev protons. Tech. rep., Air Force Weapons Laboratory.

Kaplan, A., Aydin, A., Tel, E., Sarer, B., 2009. Equilibrium and pre-equilibrium emissions in proton-induced reactions on tl-203,tl-205. Pramana-Journal of Physics 72 (2), 343–353.

Kernert, N., Peters, J. W., Schweickert, H., 1983. Test production of 201pb with protons. Jul-Spez 202, 119.

Koning, A. J., Hilaire, S., Duijvestijn, M. C., 2007. Talys-1.0.

Koning, A. J., Rochman, D., 2011. Talys-based evaluated nuclear data library version 4.

Kuhnhenn, J., Herpers, U., Glasser, W., Michel, R., Kubik, P. W., Suter, M., 2001. Thin target cross sections for proton-induced formation of radionuclides from lead for e(p) ¡= 71 mev. Radiochimica Acta 89 (11-12), 697–702.

Kurenkov, N. V., Lunev, V. P., Masterov, V. S., Shubin, Y. N., 1995. Excitation-functions for the formation of the neutron-deficient nuclei tl-201, pb-201 and bi-201 - calculated and experimental-data. Applied Radiation and Isotopes 46 (1), 29–37.

Lagunas-Solar, M. C., Jungerman, J. A., Paulson, D. W., 1980. Tl-201 yields and excitation-functions for the lead radioactivities produced by irradiation of tl-205 with 34-60 mev protons. International Journal of Applied Radiation and Isotopes 31 (2), 117–121.

Lagunas-Solar, M. C., Little, F. E., Jungerman, J. A., 1981. Proton-induced reactions on natural pb targets - a potential new cyclotron method for t1-201 production. International Journal of Applied Radiation and Isotopes 32 (11), 817–822.

Lagunas-Solar, M. C., Little, F. E., Jungerman, J. A., Peak, N. T., Theus, R. M., 1978. Thallium-201 yields and excitation functions for the lead induced radioactivities produced by irradiation of natural thallium with 15-60 mev protons. Int. J. Appl. Radiat. Isot. 29, 159–165.

Lebowitz, E., Greene, M. W., Fairchild, R., Bradleymoore, P. R., Atkins, H. L., Ansari, A. N., Richards, P., Belgrave, E., 1975. Tl-201 for medical use .1. Journal of Nuclear Medicine 16 (2), 151–155.

Malinin, A. B., Kozlova, M. D., Sevastyanova, A. S., Kharlamov, V. T., Chursin, G. P., Kochetkov, V. L., Gladun, V. T., Chumikov, G. N., Krasnov, N. N., Konyakhin, N. A., Kulygin, V. M., Abdukayumov, M. A., 1984. Production of no-carrier-added tl-201. International Journal of Applied Radiation and Isotopes 35 (7), 685–687.

Mihailescu, D., Nechifor, C.-D., Straticiuc, M., Bercea, M., 2007. Cross sections and protons optimum energy ranges for some medical radioisotopes production. Tech. rep., STIINÅ¢IFICE ALE UNIVERSITÅ¢II AL. I. CUZA IAÅI.

Milazzo-Colli, L., Braga-Marcazzan, G. M., Milazzo, M., 1975. Further measurements of probability of alpha-cluster pre-formation by means of (p, alpha) reactions in heavy elements. Nuovo Cimento Della Societa Italiana Di Fisica a-Nuclei Particles and Fields 30 (4), 632–652.

Nayak, D., Lahiri, S., Ramaswami, A., 2002. Alternative radiochemical heavy ion activation methods for the production and separation of thallium radionuclides. Applied Radiation and Isotopes 57 (4), 483–489.

Nowotny, R., 1981. Calculation of proton-induced radioisotope production yields with a statistical-model based code. International Journal of Applied Radiation and Isotopes 32 (2), 73–78.

NuDat, 2011. Nudat 2.5 database http://www.nndc.bnl.gov/nudat2/.

of-Weights-and Measures, I.-B., 1993. Guide to the expression of uncertainty in measurement, 1st Edition. International Organization for Standardization, Genve, Switzerland.

Pritychenko, B., Sonzogni, A., 2003. Q-value calculator.

Qaim, S. M., 2001. Nuclear data relevant to the production and application of diagnostic radionuclides. Radiochimica Acta 89 (4-5), 223–232.

Qaim, S. M., Weinreich, R., Ollig, H., 1979. Production of 201tl and 203pb via proton-induced nuclear-reactions on natural thallium. International Journal of Applied Radiation and Isotopes 30 (2), 85–95.

Rurarz, E., 1994. Excitation functions and yields of proton induced reactions at intermediate energies leading to important diagnostics radioisotopes of 52fe, 77br, 82rb, 97ru, 111in, 123i, 127xe, 128cs, 178ta and 201tl. Tech. rep., Soltan Institute for Nuclear Studies, SINS.

Sakai, M., Ikegama, H., Yamazaki, T., Saito, K., 1965. Nuclear structure of hg200. Nuclear Physics 65, 177–202.

Sattari, I., Aslani, G., Dehghan, M. K., Shirazi, B., Shafie, M., Shadanpour, I. N., Winkel, P., 2003. Dependence of quality of thallium-201 on irradiation data. Iran. J. Radiat. Res. 1, 51–54.

Sheu, R. J., Jiang, S. H., Duh, T. S., 2003. Evaluation of thallium-201 production in iner's compact cyclotron based on excitation functions. Radiation Physics and Chemistry 68 (5), 681–688.

Shubin, Y. N., 2001. Model calculations and evaluation of nuclear data for medical radioisotope production. Radiochimica Acta 89 (4-5), 317–324.

Shubin, Y. N., Lunev, V. P., Konobeyev, A. Y., Dityuk, A. I., 1998. Mendl-2p protonreaction data library for nuclear activation (medium energy nuclear data library). Tech. rep., IAEA.

Szelecsényi, F., Boothe, T. E., Tavano, E., Fenyvesi, A., Tárkányi, F., 1995. Evaluation of cross sections / thick target yields for 201tl production. In: Link, J. M., R.-T. J. (Ed.), Sixth Workshop on Targetry and Target Chemistry. TRIUMF, Publishing Office, p. 127.

Takács, S., Tárkányi, F., Hermanne, A., 2005. Validation and upgrading of the recommended cross-section data of charged particle reactions: Gamma emitter radioisotopes. Nuclear Instruments & Methods in Physics Research Section B-Beam Interactions with Materials and Atoms 240 (4), 790–802.

Tárkányi, F., Takács, S., Gul, K., Hermanne, A., Mustafa, M. G., Nortier, M., Oblozinsky, P., Qaim, S. M., Scholten, B., Shubin, Y. N., Youxiang, Z., 2001. Beam monitor reactions (chapter 4). charged particle cross-section database for medical radioisotope production: diagnostic radioisotopes and monitor reactions. Tech. rep., IAEA.

Tel, E., Sahan, M., Aydin, A., Sahan, H., Ugur, F. A., Kaplan, A., 2011. The Newly Calculations of Production Cross Sections for Some Positron Emitting and Single Photon Emitting Radioisotopes in Proton Cyclotrons. InTech, http://www.intechopen.com/books/radioisotopes-applications-in-physical-sciences/the-newly-calculations-of-production-cross-sections-for-some-positron-emitting-and-single-photon-emi.

Wauters, G., Vandecasteele, C., Strijckmans, K., Hoste, J., 1987. Determination of cadmium, thallium and lead in environmental-samples by proton activation-analysis. Journal of Radioanalytical and Nuclear Chemistry-Articles 112 (1), 23–31.

Zaitseva, N. G., Kovalev, A. S., Knotek, O., Khalkin, V. A., Ageev, V. A., Klyuchnikov, A. A., Linev, A. F., 1987. Preparing 201tl from lead bombarded by protons of energy about 65 mev. Soviet Radiochemistry 29 (2), 235–240.